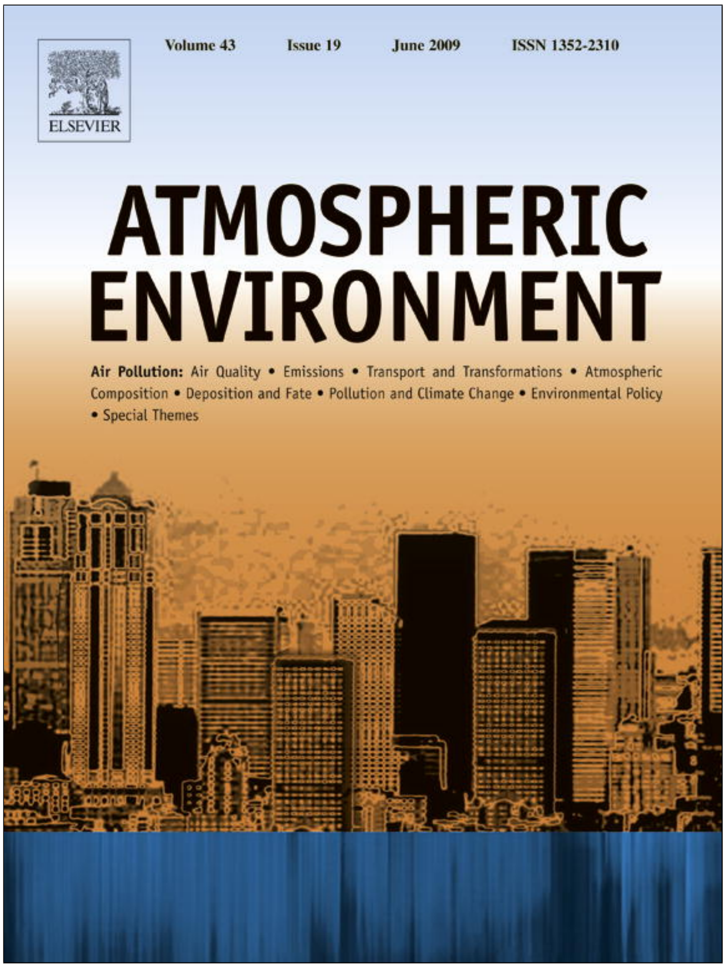

Volume 43 Issue 19 June 2009 ISSN 1352-2310

ATMOSPHERIC ENVIRONMENT

Air Pollution: Air Quality • Emissions • Transport and Transformations • Atmospheric Composition • Deposition and Fate • Pollution and Climate Change • Environmental Policy • Special Themes

Atmospheric Environment 43 (2009) 3130–3136

Contents lists available at ScienceDirect

Atmospheric Environment

journal homepage: www.elsevier.com/locate/atmosenv

Effect of different types of clouds on surface UV-B and total solar irradiance at southern mid-latitudes: CMF determinations at Córdoba, Argentina

María Laura López, Gustavo G. Palancar*, Beatriz M. Toselli*

Departamento de Físico Química/INFIQC/Centro Láser de Ciencias Moleculares, Facultad de Ciencias Químicas, Universidad Nacional de Córdoba, Ciudad Universitaria, 5000 Córdoba, Argentina

ARTICLE INFO

Article history:
Received 23 September 2008
Received in revised form
18 February 2009
Accepted 26 February 2009

Keywords:
Clouds properties
Cloud modification factor
Córdoba
Radiative transfer model
Irradiance measurements

ABSTRACT

The effect of clouds on total and UV-B irradiance in Córdoba, Argentina, was studied employing the TUV 4.1 model and measurements obtained with YES UVB-1 and YES TSP-700 radiometers, and a spectral radiometer Ocean Optics USB-4000. The experimental measurements were selected from a 10 years dataset (1999–2008). Clouds were classified by direct observation as cirrus, cumulus, and stratocumulus. The broadband Cloud Modification Factors (CMFs) have been calculated in the range of the total and the UV-B radiation for these types of clouds. The relations between them were analyzed for a significant number of days. The broadband CMF values range from around 0.1 up to 1.25, depending on the wavelength interval and on the cloud type. The CMF_{UVB} versus CMF_T plots for different clouds have shown good adjustments and significant differences, which allows the distinction between them.
Stratocumulus clouds show large attenuations and a linear relation with larger slopes as the solar zenith angle (SZA) increases. For this type of clouds an average slope of (1.0 ± 0.2) was found. The relation between the CMF for cumulus clouds is linear with an average slope of (0.61 ± 0.01). No dependence with the SZA was observed. Cirrus clouds plots show an exponential behavior with fit parameters equal to (0.48 ± 0.08) and (0.68 ± 0.15). However, when small SZA intervals are analyzed a linear relation is found. When the relations between the CMF were similar (cumulus and cirrus), the spectral variation in the UV range (320–420 nm) of a modified CMF (CMF_m) was used to distinguish them. Hence, the spectral differences among the three types of clouds have been also analyzed for several days and SZA. Here, it was found that the effect of cirrus is essentially wavelength independent while cumulus and stratocumulus clouds show exponential decay relations but with different ordinates.
In the analyzed relations the microphysical properties of the clouds seem to determine its behavior while the optical thickness leads to the different degrees of attenuation.
The results obtained in this work are in agreement with those found for other authors.

1. Introduction

UV sunlight drives the chemistry of the troposphere. As such, it is important to understand the magnitude and variability of the solar irradiance reaching the ground and the mechanisms that controls its transmission in the atmosphere. In order to assess the amount of UV radiation reaching a specific place at the Earth's surface a number of factors should be considered. Clouds are one of the most important factors influencing radiation, and consequently the photolysis rate constants. Because clouds are formed by water droplets or ice crystals, radiation is scattered when passing through them, resulting in extinction or in a diminished atmosphere transmissivity. McKenzie et al. (1996) reported attenuations of 25–30% in the global UV reaching the ground; Lubin et al. (1998) found attenuations of 10–25% in the rain forest, and Estupiñán et al. (1996) noted that attenuation may be undetectable for very thin clouds or small cloud amount but may be as high as 99% under extremely thick clouds. Moreover, Ziemke et al. (1998) stressed the importance of cloud effects in day-to-day variability of UV levels at the surface. On the other hand, ground level radiation may be affected by clouds in such a manner that it can be higher than radiation in cloudless conditions. This effect is known as broken clouds (e.g. Estupiñán et al., 1996).

The effects of clouds on the solar UV radiation are difficult to predict due to its variability and the difficulties in properly describing its characteristics. Nevertheless, it cannot be neglected because the variability induced on UV radiation is particularly

---

* Corresponding authors. Fax: +54 351 4334188.
E-mail addresses: palancar@fcq.unc.edu.ar (G.G. Palancar), tosellib@fcq.unc.edu.ar (B.M. Toselli).

1352-2310/$ – see front matter © 2009 Elsevier Ltd. All rights reserved.
doi:10.1016/j.atmosenv.2009.02.065

significant when short timescales are involved (Calbó et al., 2005). As a consequence, different theoretical and empirical parameterizations have been proposed to quantifying its effects. Many of them aim to consider a partially cover sky but they are usually based on the characteristics of the average clouds present at the location. As a result, they should be viewed as highly approximate and applicable only to the specific place. The different empirical studies of the cloud effects on UV radiation have been reviewed in Calbó et al. (2005). An example of a widely used empirical parameterization is the Cloud Modification Factor (CMF) defined in general as the ratio between the radiation for a cloudy sky and the radiation for a clear sky (which means without either clouds or aerosols). There are many historical references for the use of CMF. Paltridge and Barton (1978) related the CMF with different cloud types but they found the same behavior. Josefsson (1986) related the CMF in the UV range with the cloud cover. Ilyas (1987), Lubin and Frederick (1991), and Bais et al. (1993) found a large dispersion in the CMF for the same cloud cover. They also found differences among averaged CMF for different climates (related to different cloud types). Blumthaler et al. (1994) considered a classification of cloud types according to their altitude, distinguishing between cases when the sun was obscures by clouds or not. Schafer et al. (1996) studied the dependence of the CMF with cloud amount and with the solar zenith angle (SZA). Thiel et al. (1997) grouped their records in five categories: high clouds, altocumulus and altostratus, stratocumulus, cumulus and cumulonimbus finding that the higher the cloud liquid water content, liquid water path, or optical depth, the lower the CMF. In a previous work, Palancar and Toselli (2002) calculated the CMF but without distinguishing the type of cloud.

In the last decade, the CMF spectral studies have gained importance. Earlier papers concluded that the scattering of UV radiation by clouds is essentially wavelength independent (Josefsson and Landelius, 2000). Later papers present mainly wavelength dependent cases, as well as examples of UV enhancement showing an increasing trend with wavelength. Schwander et al. (2002) showed that, for overcast conditions, the CMF increases with decreasing wavelengths. Sabburg and Long (2004) observed spectral differences depending if the sun is occluded or not. Crawford et al. (2003) arrived to similar results but working with actinic flux ratios. Monks et al. (2004) used the slope of the CMF versus wavelength plot in a UV range to calculate the Cloud Transmittance Slope (CTS) which, in turns, was used to quantify the cloud effects. Sabburg and Parisi (2005) studied the relation between the CMF spectral dependence with the cloud cover and with the SZA. The CMF has also been used to study biological effects. Parisi et al. (2007) used CMF to assess the horizontal plane cataract effective UV irradiances. In summary, it is known that the irradiance is reduced by clouds, but it is unclear if the reduction is uniform with respect to wavelength and what is the role of the SZA and the cloud coverage.

It is known that cloud attenuation depends on a combination of different cloud properties such as cloud optical thickness, size drop or ice distribution, relative position of the sun, cloud type, number of cloud layers, liquid or ice water content, cloud cover, etc. That is why, in general, the magnitude of the attenuation itself (i.e. CMF) does not give any information about the type of cloud producing this attenuation. However, due to their singular properties every kind of cloud interacts in a different way with radiation. The previously mentioned works make reference to generic classifications and not to a unique type of cloud and, as such, this information cannot be obtained.

By considering the relation between the CMF_T and CMF_{UVB} (attenuations or increments) for different wavelength ranges, valuable information about the cloud type can be retrieved. This work analyzes the effect of the different types of clouds on surface UV-B and total irradiances through the CMF and how this factor can be used to differentiate them. Although spectral measurements provide more information, the broadband measurements are by far more common. Thus, in this work, both broadband and spectral CMF were calculated and analyzed for isolated stratocumulus, cumulus, and cirrus clouds. They were selected, in this first instance, because they are the most common at Córdoba. Although measurements were carried out at a specific site, this work is aimed to contribute to the study of the effect of clouds on radiation in the Southern Hemisphere, where measurements are by far less common than in the Northern Hemisphere. The final aim is to incorporate the properties of specific clouds in radiative transfer models to evaluate atmospheric photolysis reactions in real atmospheres.

2. Data

Three instruments were used in this work. A pyranometer YES (Yankee Environmental System, Inc.) model UVB-1, a pyranometer YES model TSP-700, and a spectroradiometer Ocean Optics USB4000. The instruments are mounted on a wide-open area in the University Campus in Córdoba City (Argentina, 31°24′S, 64°11′W, 470 m a.s.l.), which can be considered as a semi urban location. The YES UVB-1 measures UV-B global irradiance (280–315 nm) while the TSP-700 measures total global irradiance (300–3000 nm). Broadband observations are recorded as half a minute average values to assure to capture the fast cloud variability. The measurement site and the UVB-1 spectral response function have been discussed in greater detail elsewhere (Olcese and Toselli, 1998; Palancar and Toselli, 2002, respectively). Due to the fact that visible and infrared wavelengths are more sensitive to cloud presence than the UV-B wavelengths, the total irradiance measurements were used to double check the cloudy condition at all times. It is especially important when thin cirrus clouds are present to avoid being confused with a high load of aerosols (a fact common in Córdoba in wintertime; see Palancar and Toselli, 2004b). The used broadband measurements were selected from a dataset which includes measurements since 1998. The spectroradiometer measures horizontal irradiance (using a 300 μm optical fiber and an Ocean Optics CC-3 cosine corrector) between 178 and 880 nm with an optical resolution of 1.33 nm FWHM. Each measure was acquired as a 10 spectra average with 20 or 25 ms integration time.

The clouds were classified by direct observation as cirrus, cumulus, and stratocumulus. Only days with a unique type of cloud have been used in the analysis. This greatly reduces the number of days under investigation but assure that the unique responsible for the observed effect is the type of cloud under study. Besides, this condition allows analyzing its effect for different SZA, although it implies to assume that, in average, the cloud properties remained constant all day long. In the same manner, it has to be assumed that aerosol optical depth was low and the ozone level remained relatively constant during the day.

3. Model calculations

The Tropospheric Ultraviolet and Visible (TUV) radiation model version 4.1 was used for all UV-B calculations (Madronich, 1987). A sensitivity analysis was carried out using this model in order to establish the best values for the most important parameters in the calculations for Córdoba City (Palancar, 2003). The final setup used in the model was as follows: the wavelength grid was built with 1 nm intervals between 280 and 315 nm; the surface albedo was assumed to be Lambertian, wavelength independent, and with a constant value of 0.05 throughout the year; the extraterrestrial irradiance values were taken from Van Hoosier et al. (1987) and Neckel and Labs (1984). An 8-stream discrete ordinate method and cloudless sky conditions were used. Due to the low levels of tropospheric UV-B absorbing pollutants like O_3, SO_2, and NO_2 in

Córdoba City (Olcese and Toselli, 2002), they have not been considered in the calculations. Aerosols were not included. Total ozone column values were obtained daily by the Total Ozone Mapping Spectrometer (TOMS) instrument onboard Earth Probe spacecraft and were provided by the Ozone Processing Team of the Goddard Space Flight Center of the National Aeronautic and Space Administration (NASA, United States).

Total irradiance was calculated by using the α_1 and α_2 coefficients of the Kasten and Czeplak (1980) parameterization where these coefficients are, respectively, the slope and the ordinate of a plot of total irradiance versus the cosine of the SZA. To build this plot 39 clear sky days (throughout the year) taken from the 1998–2008 period were used.

To test the agreement between measurements and their corresponding models, 28 clear sky days along different years (over 25 000 data) were used. For SZA smaller than 70°, TUV showed an agreement better than ±10% while for the total irradiance parameterization it was found to be better than ±5% (Palancar and Toselli, 2004a).

4. Results and discussion

The studies of the broadband and spectral CMF are addressed in the Sections 4.1 and 4.2, respectively. In each section stratocumulus, cumulus, and cirrus clouds are analyzed. In the former, the variation of the CMF with the SZA is also analyzed while in the latter only some particular SZAs are considered.

4.1. Broadband CMF

In this study the broadband CMF was specifically defined as:

$$\mathrm{CMF}_{\mathrm{UVB}} = \frac{\mathrm{UVB}_{\mathrm{cloudy}}}{\mathrm{UVB}_{\mathrm{clear\ sky}}} \tag{1}$$

$$\mathrm{CMF}_{\mathrm{T}} = \frac{\mathrm{T}_{\mathrm{cloudy}}}{\mathrm{T}_{\mathrm{clear\ sky}}} \tag{2}$$

where UVB and T denote global UV-B and total irradiances, respectively.

As a reference, Fig. 1 shows the measurement-model ratio for one clear sky day (11/11/99) with the SZA range used for the cloudy days (14°–70°).

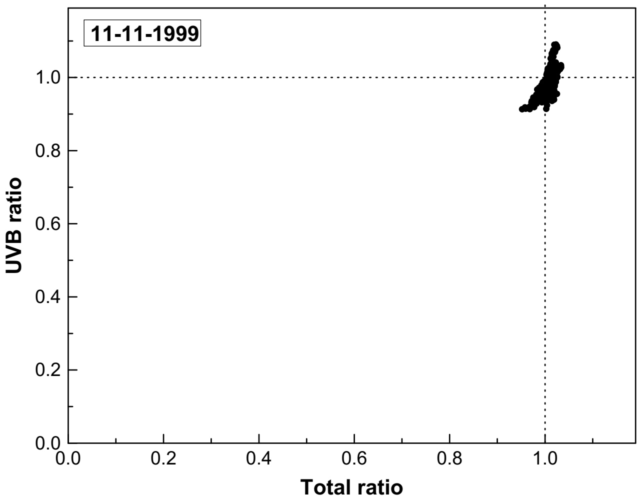

Fig. 1. UVB measurement-model ratio versus Total measurement-model ratio for a clear sky day and SZA smaller than 70°.

Figs. 2–4 show the $\mathrm{CMF}_{\mathrm{UVB}}$ as a function of $\mathrm{CMF}_{\mathrm{T}}$ for cloudy days with presence of stratocumulus, cumulus, or cirrus clouds, respectively. To study the SZA dependence, the CMF values were plotted in different symbols, each corresponding to a 5° interval of SZA. Only SZA smaller than 70° were considered due to the known uncertainties which affect models and measurements at larger SZA. The smallest SZA on each day was determined by the date of the year and the latitude of Córdoba.

4.1.1. Stratocumulus

Stratocumulus clouds are low, relatively uniform, and layered clouds with some vertical development and drop effective radius smaller than ca. 8 μm (e.g. Pawlowska et al., 2000). Fig. 2a and b shows the relations between both CMF for two different days (8/15/2001–10/13/2000, respectively) where stratocumulus clouds were present along the whole day. In both plots linear relations are clearly observed with slopes of (1.196 ± 0.008) and (1.33 ± 0.01), and correlation coefficients (R) of 0.981 and 0.968, respectively. In total, seven complete days with stratocumulus were analyzed (6207 points) obtaining an average slope of 1.0 with a standard deviation of 0.2 and an average correlation coefficient (R) of 0.97. In general, the $\mathrm{CMF}_{\mathrm{UVB}}$ values range from 0.1 to 0.7, which implies always attenuations of, at least, 30%. The $\mathrm{CMF}_{\mathrm{T}}$ are even smaller with minima around 0.1 and maxima between 0.5 and 0.6, what demonstrates a larger effect on the total irradiance than on the UV-B irradiance. This fact also reveals the high optical depth of

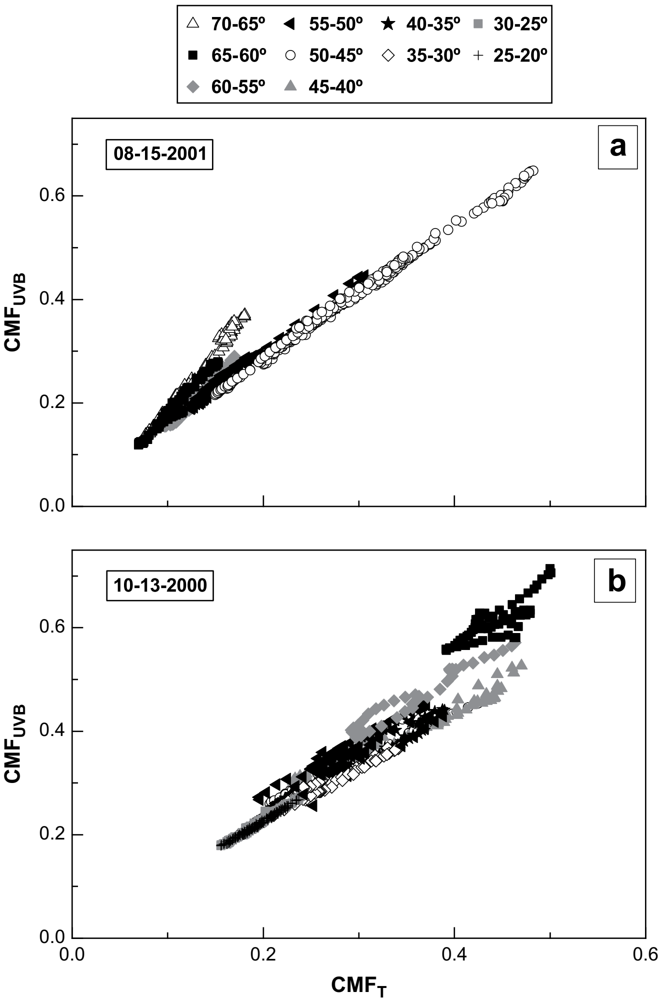

Fig. 2. $\mathrm{CMF}_{\mathrm{UVB}}$ versus $\mathrm{CMF}_{\mathrm{T}}$ for two days where stratocumulus clouds were present. The slopes of the linear fits are: a) (1.196 ± 0.008) and b) (1.33 ± 0.01).

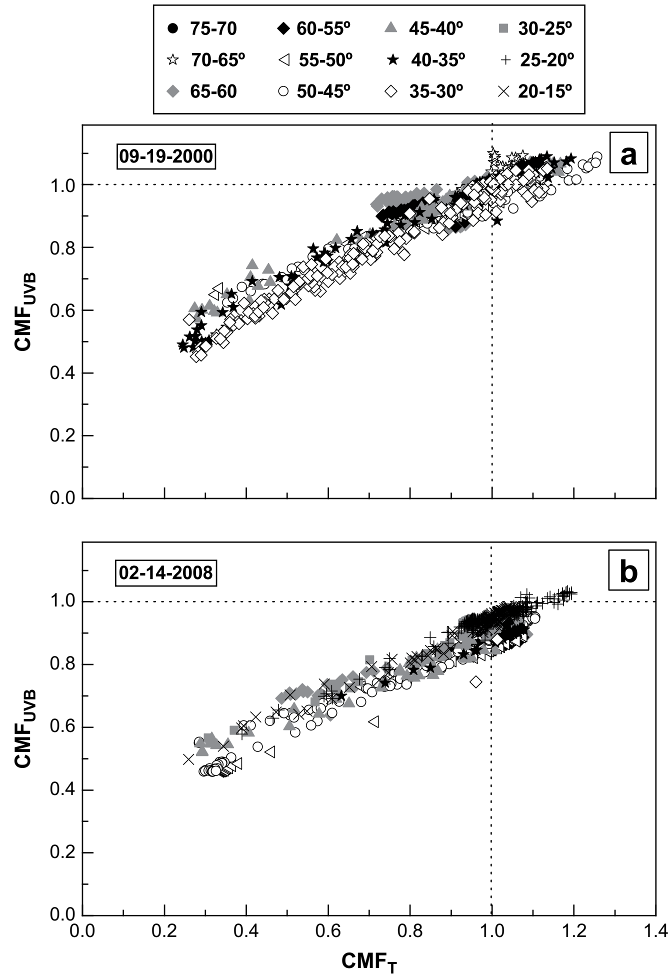

Fig. 3. CMF$_{UVB}$ versus CMF$_T$ for two days where cumulus clouds were present. The slopes for the linear fits are: a) (0.595 ± 0.006) and b) (0.612 ± 0.006).

this kind of clouds. In Fig. 2a the SZA dependence for angles between 45° and 70° can be observed. In general, it can be stated that the larger the SZA, the higher the slope. This dependence is more evident at larger SZA. Considering that the cloud field was nearly homogenous, this effect may be attributed to the increased optical depth at larger SZA. For SZA greater than 70° the irradiance values are very small and, consequently, the errors are large. This is translated into a high dispersion in the CMF plots. As an example, the SZA dependence observed for 08/15/2001 is quantified in Table 1, where the slopes and the correlation of the linear fits are shown. It should be noticed that in every SZA interval, data from the morning and from the afternoon are included. Thus, the good correlation and the little dispersion in the data for each SZA interval confirm that the type of cloud and its properties were kept nearly constant along the day and that the changes in the slopes are directly related to the SZA. The SZA dependence is not observed in Fig. 2b (where SZA between 23° and 67° are shown), probably due to a less homogenous cloud field of the stratocumulus present on this day. This fact is supported by the dispersion observed in the linear fits of some SZA intervals (not shown).

4.1.2. Cumulus

Cumulus clouds considered in this study were those classified as ordinary or fair weather. They are low clouds with small diameters, relative large liquid water content, little vertical development, and drop sizes smaller than 30 μm (Pruppacher and Klett, 1997). Fig. 3a and b shows two different days where cumulus clouds were present along the whole day (09/19/2000 and 02/14/2008, respectively). As in the stratocumulus case, the relations between the CMF are linear with good correlation coefficients (0.944 and 0.956, respectively). Even though, stratocumulus and cumulus can be distinguished by their well differentiated slopes. The slopes for cumulus clouds shown in Fig. 3 are (0.595 ± 0.006) and (0.612 ± 0.006), respectively. Additionally, the slopes of the cumulus have shown to have a high reproducibility. When 20 complete days (19 550 points) with cumulus clouds (1999–2008) were analyzed the average slope was 0.61 with a standard deviation of 0.01 and an average correlation coefficient (R) of 0.97. This type of cloud presents CMF values from around 0.2 (which means an 80% reduction) up to 1.25 being the CMF$_T$ values generally lower (more attenuation) than the CMF$_{UVB}$ ones (in common with the stratocumulus case). Values higher than 1, which are found especially in CMF$_T$, reveal an enhancement effect. This effect, known as cloud enhancement or broken clouds, is described in various studies (e.g. Schafer et al., 1996; Sabburg and

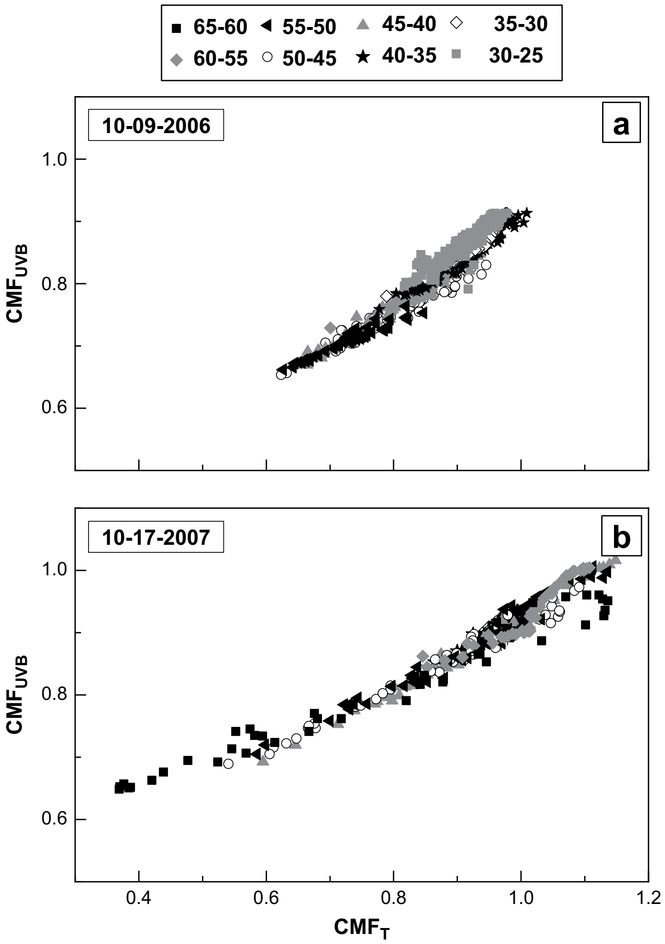

Fig. 4. CMF$_{UVB}$ versus CMF$_T$ for two days where cirrus clouds were present. See text.

Table 1
SZA dependence of the CMF$_{UVB}$ versus CMF$_T$ plot for stratocumulus clouds on 08/15/2001. See text.

SZA dependence for stratocumulus			
SZA interval (°)	Slope	Ordinate	R
70–65	2.324	−0.049	0.994
65–60	1.972	−0.022	0.981
60–55	1.766	−0.019	0.969
55–50	1.272	0.042	0.995
50–45	1.285	0.028	0.999

Wong, 2000) and in this case it reached a 25%. This effect is observed when the sun is not occluded and it is attributed to the reflections in cloud boundaries (especially for those with high vertical development such as *cumulus congestus*) or due to the fact that the diffuse radiation coming from the cloud base is higher than the diffuse radiation of the portion of the sky the cloud is blocking. In contrast with the stratocumulus, cumulus clouds show the same slope for all the SZA intervals. This behavior has been observed for SZA up to 80°. As an example, the SZA dependence observed for 02/13/2002 is quantified in Table 2, where the slopes and the correlation of the linear fits are shown. In Fig. 3a and b SZA range from 32° up to 70° and from 18° up to 67°, respectively. As can be seen, the CMF within each SZA interval vary from small values (large attenuations) up to values larger than 1. This characteristic can be explained considering two facts: the inhomogeneous vertical development within each individual cloud element and the movement of the cloud field with the wind. These two factors can produce, in a lapse of a few minutes or seconds, large changes in the optical depth. These changes are responsible for the characteristic peaks and drops in an irradiance curve when cumulus clouds are present. Values higher than 1 correspond to periods when the sun shines through the cloud elements.

If the UV-B and total measurement-model agreements were perfect, the ratio between them for a clear sky day would group around the (1;1) point as it was shown in Fig. 1. However, the agreements are not perfect and, even when the sun is not occluded, a fraction of the sky is blocked by clouds, which affect in a different way the UV-B and the total irradiance. That is why the linear array of points in Fig. 3a passes through the (1;1) point while that one on Fig. 3b does not. This behavior may be explained considering two issues, one related to the cloud–radiation interaction and the other one based on the uncertainties affecting models. When the sun is not occluded, the direct component is just the same as a clear sky day. The diffuse component, instead, will be affected in a different way depending on the cloud cover and the cloud properties. As it was previously stated, when the cloud base is brighter (i.e. it is white) than the portion of the sky the cloud is occluding the extra diffuse radiation produces the cloud enhancement (the involved approximations and equations can be seen in Nack and Green, 1974). On the other hand, when the cloud base is grey a reduction is observed. This reduction in the diffuse radiation also happens for the total radiation. However, in this case, it is negligible because the diffuse component represents only a small percentage of the global total radiation (as opposed to the UV-B case where it represents at least a 50%). The other factor is related to the agreement between the experimental measurements and their corresponding models. As it was mentioned, the total irradiance parameterization shows a better agreement than the TUV model. Besides the clouds, the other two main factors which affect radiation are aerosols and ozone. The former always produces reductions in experimental measurements while a wrong consideration of the latter can lead to overestimations or underestimations in model calculations. Nevertheless, both factors affect more the UV-B than the total radiation, leading to larger uncertainties in CMF_{UVB} than in the CMF_T. Thus, variable combinations between cloud properties and model agreements will conduct to different behaviors of the array of points respect to the (1;1) point.

The ordinates in Fig. 3a and b (0.326 and 0.318) reveal that when the total irradiance is almost completely attenuated, a significant portion of the UV-B one can be still transmitted through the clouds.

4.1.3. Cirrus

Cirrus clouds form above 6000 m, are rather thin and are composed of nonspherical ice crystals of variable habits and sizes (ranging from micrometers to millimeters) depending of their formation temperature. The relevance of cirrus clouds resides in that they are globally widespread and hence they are important modulators of incoming solar radiation and outgoing terrestrial radiation (Liou, 1986). After analyzing 12 complete days with cirrus (12 598 points in 68 SZA intervals 5° wide) it has been found that the relation between the CMF follows the form

$$CMF_{UVB} = Ae^{CMF_T \cdot t} \tag{3}$$

where A and t are fit parameters with average values of (0.48 ± 0.08) and (0.68 ± 0.15), respectively. The average correlation coefficient (R) for this fit was better than 0.93. Fig. 4a and b shows this relation for two days where cirrus clouds were present along the whole day (10/09/2006 and 10/17/2007, respectively). As can be seen, the distinction from stratocumulus and cumulus is clear. Going one step further in the analysis we found that the relation within every 5° SZA interval is linear, with higher slopes at smaller SZA. As an example, Table 3 shows the SZA dependence for 10/09/2006 (see Fig. 4a). This dependence and the fact that at larger SZA the attenuation is greater lead to the exponential behavior observed for cirrus. It is worthwhile to note here that the SZA dependence has the opposite tendency that in the stratocumulus case. Note that when measurements are available only for a small SZA interval the relation may appear as linear. In this case the problem can be overcome by resorting to the spectral CMF (see next section).

Concerning the uncertainties affecting the CMF values, many factors should be mentioned: the different rate at which the absolute calibration of every instrument changes (besides the absolute calibration itself), the ozone variations during the day, the presence of unnoticeable (for a direct observer) amounts of aerosols, and the approximations used in the TUV model. The common feature of all these factors is that they affect the two wavelength ranges in a different extent being able to change, in this way, the slope of the plots (Figs. 2–4). Nevertheless, note that these usually small uncertainties (inherent of measurements and models) will change simultaneously the CMF values producing,

Table 2
SZA dependence of the CMF_{UVB} versus CMF_T plot for cumulus clouds on 02/13/2002. See text.

SZA dependence for cumulus

SZA interval (°)	Slope	R
55–50	0.497	0.976
50–45	0.513	0.979
45–40	0.595	0.991
40–35	0.545	0.993
35–30	0.601	0.984
30–25	0.738	0.992
25–20	0.633	0.989
20–15	0.683	0.976
15–10	0.676	0.992
10–5	0.655	0.991

Table 3
SZA dependence of the CMF_{UVB} versus CMF_T plot for cirrus clouds on 10/09/2006. See text.

SZA dependence for cirrus

SZA interval (°)	Slope	R
65–60	0.23782	0.93293
60–55	0.33974	0.87786
55–50	0.36034	0.93156
50–45	0.54551	0.96497
45–40	0.63029	0.98468
40–35	0.67254	0.96033
35–30	0.73508	0.92024
30–25	0.79255	0.96015

each one, underestimations or overestimations. Thus, it is expected that in the final CMF values they will be partially compensated.

4.2. Spectral CMF

At present, it is known that the spectral intensity is reduced by clouds, but it is unclear if the reduction is uniform with respect to wavelength. The spectral CMF were calculated using a smaller dataset (measurements were started on 2007). The main purposes of this section are to complement the broadband analysis to distinguish cumulus from cirrus when both CMF relations are linear, and to shed light on the spectral dependence. This analysis is based on the wavelength dependence produced by these types of clouds. Here it is also shown the first results for this dependence produced by stratocumulus. The used wavelength range covers from 320 up to 700 nm. To avoid introducing additional changes or uncertainties in the CMF (for example the spectral dependence of the albedo) the spectral CMF calculations were based entirely on experimental data. The radiation measurements when cumulus or cirrus clouds are present allow discriminating two situations: the sun occluded or not. Thus, the periods when the sun was shining, immediately after or before a cloud occlusion, were used as a kind of clear sky measurement. This approach assures identical atmospheric conditions for both measures (cloudy and clear) avoiding the uncertainties introduced by a model through the not-measured input parameters and the possible biases due to the instrument calibration or position. The differences that can introduce the extra diffuse radiation coming from the base of the clouds (respect to the clear sky) were minimized taking measurements with the less number of clouds as possible. In these conditions it is observed that, in spite of the presence of the cloud, when the sun is not occluded the radiation immediately returns to the clear sky level (as calculated by the model). Thus, here the CMF is not a simple cloudy/clear relation. In this case the CMF is actually given by the ratio between the irradiance when the sun is occluded by the cloud and the irradiance when the sun is not occluded, remaining all the other atmospheric conditions unaltered. The analytic expression for this modified Cloud Modification Factor ($\mathrm{CMF_m}$) results as follow:

$$\mathrm{CMF_m} = \frac{\mathrm{Dir_{cloud}} + \mathrm{Dif_{cloud}} - (1-c)(\mathrm{Dif_{cloud}} - \mathrm{Dif_{sun}})}{\mathrm{Dir_{sun}} + \mathrm{Dif_{sun}} + c(\mathrm{Dif_{cloud}} - \mathrm{Dif_{sun}})} \qquad (4)$$

where c is the cloud cover, Dir and Dif are the direct and diffuse components and the cloud and sun subscript make reference to the situations when the sun is occluded and not occluded, respectively. Note that numerator and denominator represent the extreme values during a cloudy day: when the irradiance is lower than it is on an overcast day and when it is higher than it is on a clear sky day, respectively (refer to Nack and Green, 1974 or Lantz et al., 1996 to see a complete deduction of these expressions). In this way, the effect of the cloud is amplified, canceling, at the same time, all the other differences due to the changing or unknown atmospheric conditions.

Fig. 5 shows the spectral $\mathrm{CMF_m}$ obtained for the day showed in Fig. 4b (cirrus on 10/17/2007) and for the day with cumulus showed in Fig. 3b (02/14/2008). The curve for cirrus was taken at an SZA equal to 38°, while the cumulus curve corresponds to an SZA equal to 28°. As can be seen in Fig. 5 the wavelength dependences are visibly different. Cirrus clouds show a linear fit with a slope in the order of 10^{-6} with an ordinate equal to 0.88. That means that they produce an attenuation close to 10% and essentially wavelength independent. On the other hand, cumulus clouds show a significant wavelength dependence. The $\mathrm{CMF_m}$ decreases from 0.7 up to 0.57 (from 320 to 700 nm) with a first order exponential decay dependence ($R = 0.971$). Hence, the spectral dependence allows making a clear distinction between cumulus and cirrus when they present a similar relation between $\mathrm{CMF_{UVB}}$ and $\mathrm{CMF_T}$ (i.e. when the SZA interval available is small the relation for cirrus may seem lineal). In order to verify and generalize this analysis cumulus and cirrus measurements for other days and SZA were examined finding the same behavior: very small slopes and attenuations within the 10% for cirrus and larger attenuations with an exponential dependence for cumulus. In both cases the degree of attenuation is certainly related with the optical depth.

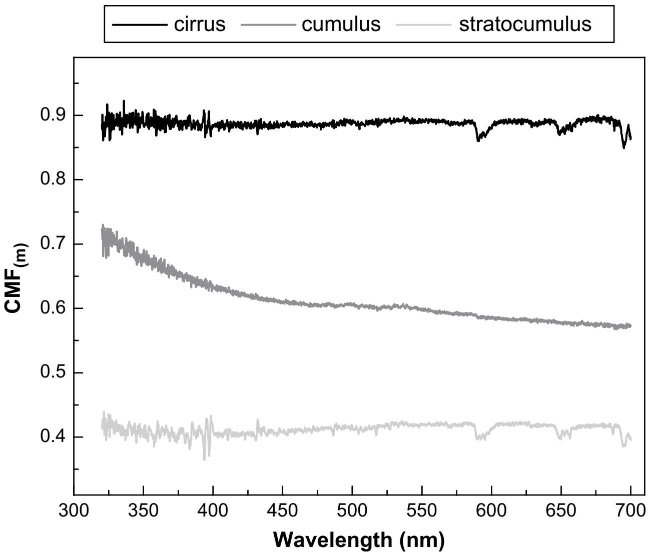

Fig. 5. $\mathrm{CMF_m}$ as a function of wavelength for cirrus and cumulus. In the stratocumulus case the CMF was calculated. See text.

In other works, the slopes of the spectral CMF were used to quantify the effect of clouds on radiation (Schwander et al., 2002; Crawford et al., 2003; Monks et al., 2004; Sabburg and Parisi, 2005) though using different radiative magnitudes and/or settings to build the CMF (actinic flux or irradiance, wavelength range, experimental clear sky or model calculations, etc.). Despite these differences, and regardless of the SZA, the slopes in the (320–420 nm) wavelength interval obtained in this study were comparable to those in the other studies (negative slopes with an order of magnitude equal to 10^{-3} and average $R > 0.97$).

Finally, Fig. 5 also shows the spectral variation of the irradiance when stratocumulus clouds are present (10/26/2007). As these clouds do not allow the sun to shine between the individual elements, a measurement at the same SZA on the previous clear sky day was used as reference. Hence, in this case the ratio corresponds to cloudy/clear relation (CMF). Even though the variation at wavelengths longer than 450 nm is similar to that of cumulus, these clouds can be differentiated through their slopes in the UV range because stratocumulus clouds show negative slopes in the order of 10^{-4}. Given that cirrus clouds exhibit comparable slopes the division from them can be done considering their ordinates, inasmuch as stratocumulus clouds usually produce larger attenuations.

In spite of no physical considerations were addressed in this work, an explanation widely accepted is that the spectral effects induced by clouds are because the radiation is reflected and then scatters downward again by the Rayleigh scattering. Because of the increase of the optical depth, due to the air molecules, with the decrease of the wavelength these photons have a higher chance to be scattered downward again (Kylling et al., 1997).

5. Conclusions

In this paper, the effect of different type of clouds (stratocumulus, cumulus, and cirrus) on surface irradiance has been investigated. Experimental measurements and model calculations (TUV 4.1) were used to study the relation between the CMF_{UVB} and CMF_T and the spectral variation of a modified CMF (CMF_m).

The observed features of the CMF_{UVB} versus CMF_T plot for the three different types of clouds allow the distinction among them. They can be summarized as follow:

a. Stratocumulus clouds show CMF smaller than 0.7 for both irradiances (being the CMF_T smaller than the CMF_{UVB}) and a linear relation with an average slope of (1.0 ± 0.2). The SZA dependence shows that the larger the SZA, the larger the slope.
b. Cumulus clouds show CMF ranging from around 0.2 up to 1.25 (broken clouds), especially for total irradiance. The relation between the CMF is linear with an average slope of (0.61 ± 0.01). No dependence with the SZA could be observed.
c. Cirrus clouds show CMF from around 0.6 up to values close to 1. The relation between the CMF is exponential. However, within each 5° SZA interval, the relations are linear with lower slopes and stronger attenuations at larger SZA. When both kinds of radiation measurements are not available the found relations allow to infer the effect of a specific type of cloud on the missing one.

When the found relations are similar (i.e. for cumulus and cirrus) the spectral variation of modified CMF (CMF_m) can be used to distinguish them. While cirrus clouds show weak attenuations and a variation essentially independent of wavelength, cumulus clouds show an exponential decay relation. When the (320–420 nm) wavelength interval is analyzed for cumulus, linear relations with negative slopes are found. Although stratocumulus clouds also show negative slopes they can be differentiated by their larger attenuation. Hence, the microphysical properties of the cloud seem to determine its behavior while the optical thickness leads to the different observed attenuations.

In summary, the combination of model calculations and broadband (UV-B and total) and spectral irradiance measurements allows to distinguish the type of cloud producing a given attenuation. All the results in this work apply, in first term, to typical clouds observed in Córdoba. These relations, although can be expected, may not be necessarily the same for clouds of the same type but with other properties (altitude, optical depth, morphology, drop size distribution, liquid or ice water content, etc.), especially those formed in other latitudes. Thus, more research is needed to verify and validate the presented findings. The role of the cloud coverage and the SZA on the wavelength dependence still remains open.

Acknowledgements

We thank CONICET and SeCyT (UNC) for partial support of the work reported here. María Laura López thanks Fundación YPF for a research grant that made possible her studies.

References

Bais, A.F., Zerefos, C.S., Meleti, C., Ziomas, I.C., Tourpali, K., 1993. Spectral measurements of solar UVB radiation and its relations to total ozone, SO_2 and clouds. Journal of Geophysical Research 98 (D3), 5199–5204.

Blumthaler, M., Ambach, W., Salzgeber, M., 1994. Effects of cloudiness on global and diffuse UV irradiance in a high-mountain area. Theoretical and Applied Climatology 50, 23–30.

Calbó, J., Pagès, D., González J-, A., 2005. Empirical studies of cloud effects on UV radiation: a review. Reviews of Geophysics 43, 2002–2005.

Crawford, J., Shetter, R.E., Lefer, B., Cantrell, C., Junkermann, W., Madronich, S., Calvert, J., 2003. Cloud impacts on UV spectral actinic flux observed during the International Photolysis Frequency Measurement and Model Intercomparison (IPMMI). Journal of Geophysical Research 108 (D16), 8545–8556.

Estupiñán, J.G., Raman, S., Crescenti, G.H., Streicher, J.J., Barnard, W.F., 1996. Effects of clouds and haze on UV-B radiation. Journal of Geophysical Research 101 (D11), 16807–16816.

Ilyas, M., 1987. Effect of cloudiness on solar ultraviolet radiation reaching the surface. Atmospheric Environment 21 (6), 1483–1484.

Josefsson, W., 1986. Solar Ultraviolet Radiation in Sweden. SMHI Reports Meteorology and Climatology No. 53. Swedish Meteorological and Hydrological Institute, Norrköping, Sweden.

Josefsson, W., Landelius, T., 2000. Effects of clouds on UV irradiance: as estimated for cloud amount, cloud type, precipitation, global radiation and sunshine duration. Journal of Geophysical Research 105 (D4), 4927–4935.

Kasten, F., Czeplak, G., 1980. Solar and terrestrial radiation dependent on the amount and type of cloud. Solar Energy 24, 177–189.

Kylling, A., Albold, A., Seckmeyer, G., 1997. Transmittance of a cloud is wavelength-dependent in the UV-range: physical interpretation. Geophysical Research Letters 24 (4), 397–400.

Lantz, K.O., Shetter, R.E., Cantrell, C.A., Flocke, S.J., Calvert, J.G., Madronich, S., 1996. Theoretical, actionometric, and radiometric determinations of the photolysis rate coefficient of NO_2 during MLOPEX II. Journal of Geophysical Research 101, 14613–14629.

Liou, K.N., 1986. Influence of cirrus clouds on weather and climate processes: a global perspective. Monthly Weather Review 114, 1167–1199.

Lubin, D., Frederick, J.E., 1991. The ultraviolet radiation environment of the Antarctic Peninsula: the roles of ozone and cloud cover. Journal of Applied Meteorology 30, 478–493.

Lubin, D., Chen, B., Bromwich, D.H., Somerville, R.C.J., Lee, W.-H., Hines, K., 1998. The impact of Antarctic cloud radiative properties on a GCM climate simulation. Journal of Climate 11, 447–462.

Madronich, S., 1987. Photodissociation in the atmosphere: 1. Actinic flux and the effects of ground reflections and clouds. Journal of Geophysical Research 92, 9740–9752.

McKenzie, R.L., Bodeker, G.E., Keep, D.J., Kotkamp, M., Evans, J.M., 1996. UV radiation in New Zealand: measured north to south differences, relationship to other latitudes. Weather and Climate 16, 17–26.

Monks, P.S., Rickard, A.R., Hall, S.L., Richards, N.A.D., 2004. Attenuation of spectral actinix flux and photolysis frequencies at the surface through homogeneous clouds fields. Journal of Geophysical Research 109, D17206. doi:10.1029/2003JD004076.

Nack, M.L., Green, A.E., 1974. Influence of clouds, haze, and smog on the middle ultraviolet reaching the ground. Applied Optics 12, 2405–2415.

Neckel, H., Labs, D., 1984. The solar radiation between 3300 and 12500 Å. Solar Physics 90, 205–258.

Olcese, L.E., Toselli, B.M., 1998. Unexpected high levels of ozone measured in Córdoba, Argentina. Journal of Atmospheric Chemistry 31, 269–279.

Olcese, L.E., Toselli, B.M., 2002. Some aspects of air pollution in Córdoba, Argentina. Atmospheric Environment 36, 299–306.

Palancar, G.G., 2003. Estudio de procesos cinéticos y radiativos de interés atmosférico. Ph.D. Thesis, Universidad Nacional de Córdoba, Argentina.

Palancar, G.G., Toselli, B., 2002. Erythemal ultraviolet irradiance in Córdoba, Argentina. Atmospheric Environment 36, 287–292.

Palancar, G.G., Toselli, B., 2004a. Effects of meteorology on the annual and interannual cycle of the UV-B and total radiation in Córdoba City, Argentina. Atmospheric Environment 36, 1073–1082.

Palancar, G.G., Toselli, B.M., 2004b. Effects of meteorology and tropospheric aerosols on UV-B radiation: a 4-year study. Atmospheric Environment 38, 2749–2757.

Paltridge, G.W., Barton, I.J., 1978. Erythemal Ultraviolet Radiation Distribution over Australia – the Calculations, Detailed Results and Input Data. Tech. Pap. 33. Aus. Div. of Atmos. Phys., Commonw. Sci.. and Indus. Res. Organ., Aspendale, Victoria, Australia, 48 pp.

Parisi, A.V., Turnbull, D.J., Turner, J., 2007. Calculation of cloud modification factors for the horizontal plane eye damaging ultraviolet radiation. Atmospheric Research 86, 278–285.

Pawlowska, H., Brenguier, J., Burnet, F., 2000. Microphysical properties of stratocumulus clouds. Atmospheric Research 55, 15–33.

Pruppacher, H.R., Klett, J.D., 1997. Microphysics of Clouds and Precipitation, second ed. Kluwer Academic Publishers, The Netherlands.

Sabburg, J.M., Long, C.N., 2004. Improved sky imaging for studies of enhanced UV irradiance. Atmospheric Chemistry and Physics 4, 2543–2552.

Sabburg, J.M., Parisi, A.V., 2005. Spectral dependency of cloud enhanced UV irradiance. Atmospheric Research 81, 206–214.

Sabburg, J., Wong, J., 2000. The effect of clouds on enhancing UVB irradiance at the earth's surface: a one year study. Geophysical Research Letters 27 (20), 3337–3340.

Schafer, J.S., Saxena, V.K., Wenny, B.N., Barnard, W., DeLuisi, J.J., 1996. Observed influences of clouds on ultraviolet-B radiation. Geophysical Research Letters 23 (19), 2625–2628.

Schwander, H., Koepke, P., Kaifel, A., Seckmeyer, G., 2002. Modification of spectral UV irradiance by clouds. Journal of Geophysical Research 107 (D16), 4296.

Thiel, S., Steiner, K., Seidlitz, H.K., 1997. Modification of global erythemally effective irradiance by clouds. Photochemistry and Photobiology 65, 969–973.

Van Hoosier, M.E., Bartoe, J.D., Brueckner, G.E., Printz, D.K., 1987. Solar Irradiance Measurements 120–400 nm from Space Lab-2. IUGG Assembly, Vancouver.

Ziemke, J.R., Herman, J.R., Stanford, J.L., Bhartia, P.K., 1998. Total ozone/UVB monitoring and forecasting: impact of clouds and the horizontal resolution of satellite retrievals. Journal of Geophysical Research 103 (D4), 3865–3871.